Quaternary International 355 (2015) 202–208

Contents lists available at ScienceDirect

Quaternary International

journal homepage: www.elsevier.com/locate/quaint

Forum communication

Application of logistic regression and frequency ratio in the spatial distribution of debris-rockslides: Precordillera of San Juan, Argentina

María Yanina Esper Angillieri*

CONICET, Gabinete de Neotectónica y Geomorfología, INGEO, Facultad de Ciencias Exactas, Físicas y Naturales, Universidad Nacional de San Juan, Av. José I. de la Roza y Meglioli, Rivadavia, San Juan, 5400, Argentina

ARTICLE INFO

Article history:
Available online 21 November 2014

Keywords:
Debris-rockslides
Frequency ratio
Logistic regression
Precordillera
Argentina

ABSTRACT

This study employs statistical modeling techniques and geomorphological mapping to analyze the distribution of debris-rockslides in relation to altitude, aspect, slope angle, lithology and distance to lineaments using optical remote sensing techniques with GIS. The study area includes a portion of the Central Precordillera of San Juan around 32°S, 69°W, where few geomorphological studies have been conducted. A debris-rockslides inventory map was prepared using debris-rockslides locations identified from satellite imageries, a total of 35 debris-rockslides were identified in an area of 288.13 km^2 (with a total slide area of 6.36 km^2). All of the debris-rockslides were rotational slides, affecting Upper Ordovician and Upper Devonian deposits. The volumes of debris-rockslides were estimated using the sloping local base level technique that allows computing the possible pre-rockslide topography and the bedrock–deposits interface. The relationship between the variables and the slide distribution was analyzed using the frequency ratio method and logistic regression models. The analytical results show that lithology and slope exert major influences. Lithology is found to be the most important aspect in the study area.

1. Introduction

Landsliding does not affect the Argentine population as much as other geomorphologic processes do, because only about 30% of the country's total population inhabits provinces with mountain ranges (Moreiras and Coronato, 2009). A landslide is the movement of rock, detritus, or soils caused by the action of gravity. Larger collapses may affect local watercourses and influence the activity of local communities; greater landslides may provoke disasters and change the geomorphologic setting of several square kilometers of land (Vittorio De Blasio, 2011). Debris rockslides are usually characterized by well-defined head scarps and flanks, a pronounced scar generally left with little or no debris, and a mass of debris that accumulates in the track or at the base. In a sliding rock mass, a planar slope surface is developed. If the rock slides well away from the depletion zone, the scar and flanks may remain visible (Dikau, 2004).

A landslide inventory map provides the spatial distribution of locations of existing landslides. This type of information is very important, as it gives insight into landslide location, type, dates, state of activity, magnitude or size, failure mechanisms, causal factors and damage caused (Fell et al., 2008). The factors that determine the occurrence of landslide of an area may be grouped into two categories: (1) the intrinsic variables that contribute to landslide susceptibility, such as lithology, slope gradient, aspect, elevation, vegetation cover, and drainage patterns; and (2) the extrinsic variables that tend to trigger landslides in an area of given susceptibility, such as heavy rainfall and earthquakes (Atkinson and Massari, 1998).

Between 28° and 32°S, a series of geologic and tectonic factors can be related to surface seismic activity, since these latitudes the Nazca Plate is subducing subhorizontally. In this intra-plate setting, the most important destructive earthquakes have taken place, such as the earthquakes of 1894 (Ms 7.5), 1944 (Ms 7.4) and 1977 (Ms 7.4). At these latitudes, where there is high degree of seismicity, the principal effects of earthquakes in hilly areas are landslides.

Several authors have studied landslides in Argentina. In the Precordillera. some examples are: Fauqué et al. (2000); Esper Angillieri and Perucca, 2013 and Esper Angillieri et al. (2014); on Precordillera and Cordillera Frontal: Perucca and Esper Angillieri (2008, 2009a,b) and Esper Angillieri (2011, 2012); on Cordillera Principal: González Díaz (2009) and González Díaz and Folguera (2009) and on Sierras Pampeanas: Fernández (2005).

The aim of this study is analyze the distribution of one type of landslide, the dry debris rockslides, in a sector of the Central

* Corresponding author.
E-mail address: yaninaesper@gmail.com.

http://dx.doi.org/10.1016/j.quaint.2014.11.002
1040-6182/

Precordillera of San Juan, Argentina, relative to altitude, aspect, slope angle, lithology and distance to lineaments, by analyzing topographical maps and satellite images, and using the frequency ratio and logistic regression models.

2. Regional setting

The selected area for this survey covers 435.55 km^2 and includes a portion of the Central Precordillera of San Juan, Sarmiento Department, with a central point coordinates of 31°53′S and 69°01′W, characterized by high relief with peaks up to 4300 m asl. (Fig. 1). San Juan province (Fig. 1) supports an arid and semiarid climate; the total annual rainfall average is very small, about 93.3 mm per year. Winter temperatures are generally mild, ranging between 1.0 and 18.0 °C, whereas summers are hot and very dry, with temperatures between 19.0 and 35.0 °C (Data from San Juan meteorological station 31°36′S – 68°33′20″W)'. In the study area, the annual rainfall is 280 mm. The temperature in summer reaches 39 °C (February) and in the winter −10 °C (July).

The study area supports a wide range of geologic units. The stratigraphy from oldest to recent is: (a) Cambrian-Ordovician sedimentary rocks mainly composed of limestone and dark lutite, (b) Ordovician sandstones and pelites, (c) A package of graywacke and lutites, mainly of marine origin of Devonian age, (d) Neogene

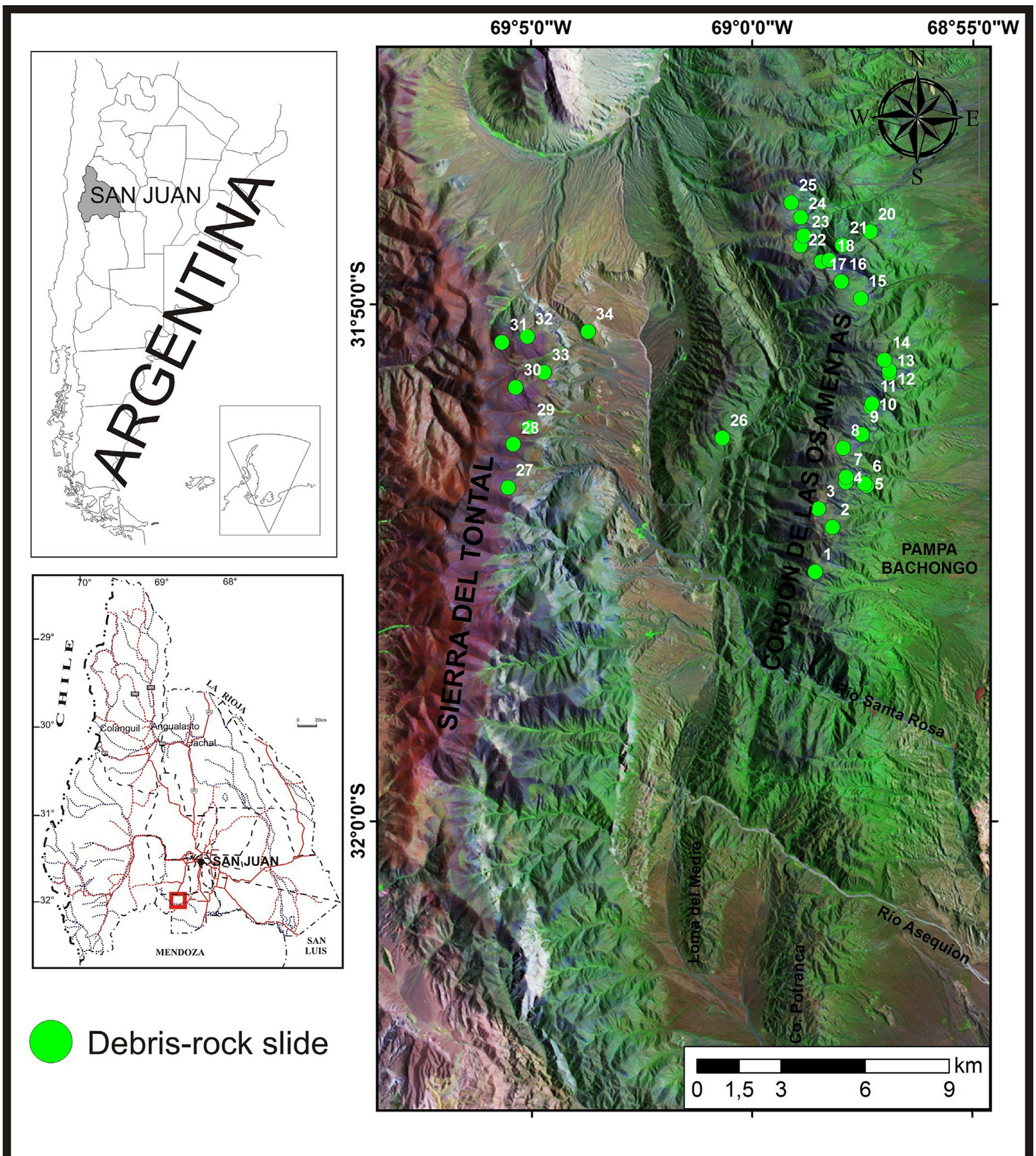

Fig. 1. Location of study area and spatial distribution of debris -rock slide.

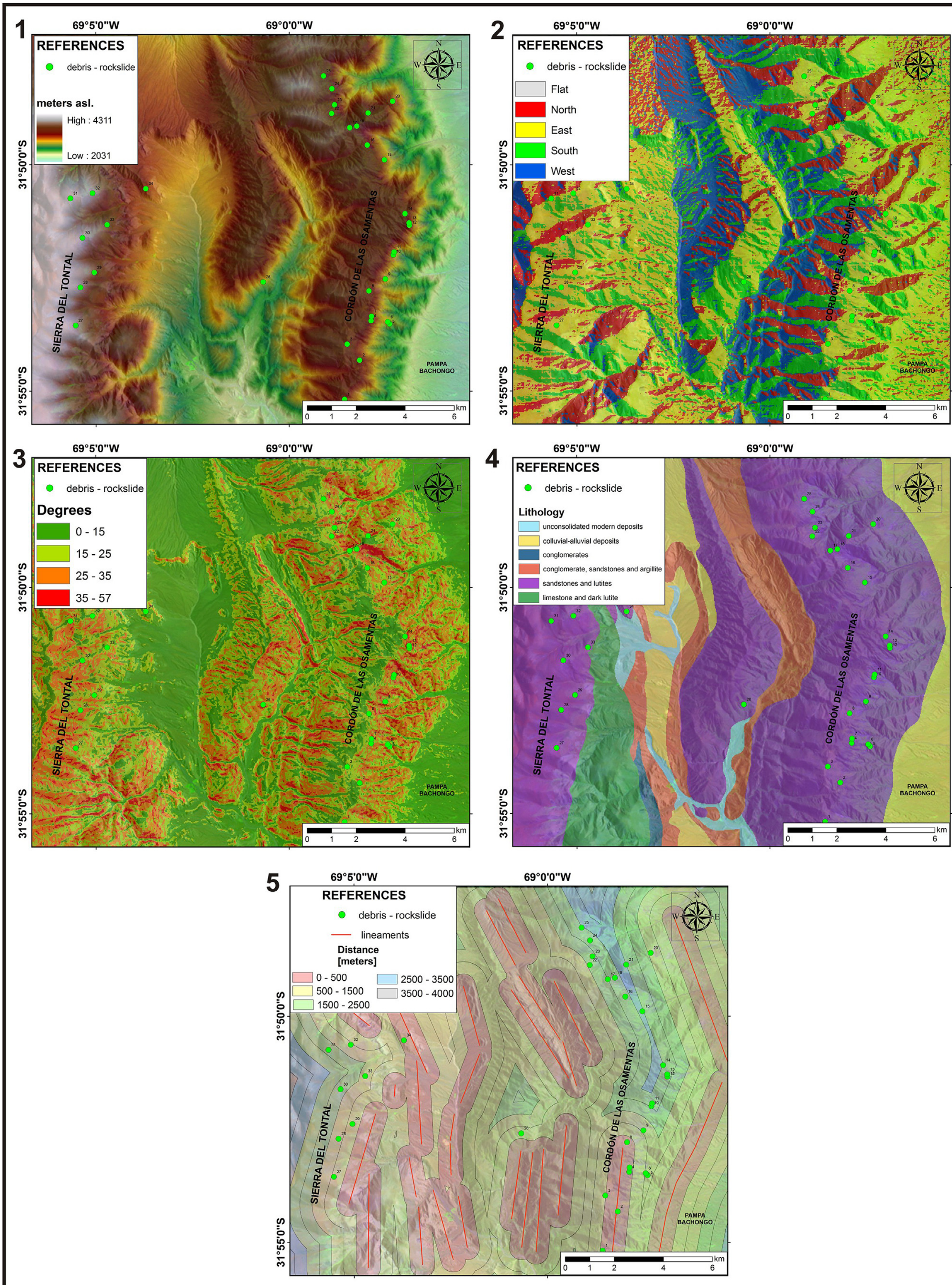

Fig. 2. Variables maps: 1) altitude, 2) slope aspect, 3) slope angle, 4) lithology and 5) distances to lineament.

sedimentary rocks (conglomerate, sandstones and argillite), (e) Quaternary colluvial-alluvial deposits, (f) Modern unconsolidated deposits, sand, silt and clay, that are restricted to narrow river channels and to the valleys.

The Central Precordillera has been described as a typical thin-skinned thrust-and-fold belt, with Neogene crustal shortening dipping west, and imbricated structures rooting down towards a 10–15 km deep main décollement (Allmendinger et al., 1990). Reverse faults with Quaternary tectonic activity are found in the eastern piedmont of the Cordón de Las Osamentas (Perucca and Onorato, 2011). All the faults are located at a distance between 2 and 20 km from the debris rockslides area. N–S trending thrust faults affect the lower or distal part of the alluvial fans, east-facing scarps up to 10-m high define the fault trace.

3. Materials and methods

An inventory of debris rockslides in the study area was prepared in order to identify their relationships with conditional factors such as altitude, aspect, slope angle, lithology, and distance to lineaments. The debris rockslides were identified using high resolution satellite imagery (SPOT 5 with a 2.5-m spatial resolution, taken in August 2002 and January 2003) from Google Earth™, which were georeferenced to a geographical coordinate system (WGS84) within a geographical information system (GIS). The identified debris-rockslides and their areas were stored, in vector format, through manual digitalization using GIS.

Elevations (Fig. 2) were obtained from topographical information obtained from ASTER GDEM V2 (NASA, 2011). Therefore, a digital elevation model (DEM) was made for the region. Using the DEM, slope aspect (Fig. 2) and the slope angle (Fig. 2) were calculated. The lithology (Fig. 2) data were acquired from geologic map sheets (3169-III Barreal, preliminary and 3169-IV San Juan) published by the Servicio Geológico Minero Argentino (Argentine Mining Geologic Service) at 1:250,000 scale (SEGEMAR, 2000).

Fault lines and lineaments located in the study area were derived by integrating the existing geological data and imagery interpretation. The study area and its vicinity are significantly affected by the Neotectonic activity of the region; these data strongly suggest the role of fault zones in controlling the distribution of landslide scars (Perucca and Onorato, 2011). Therefore, to assess cause–effect relationships between lineaments and slide occurrence, distances to lineaments (Fig. 2) was calculated using multiple buffers of 100 m incremental distance. The morphometric parameters of the debris-rockslides were measured according to the definitions to WP/WLI *(International Geotechnical Societies = UNESCO Working Party on World Landslide Inventory)* suggested Nomenclature for Landslides (modified of IAEG, 1990).

In order to compute the volume of the debris-rockslides, the pre-slide topography needs to be reconstructed. This reconstruction is based on the continuity between the present topography outside the scar area and the pre-event topography within the slide area. The pre-slide DEM was obtained by reshaping post-slide DEM, by deleting points corresponding to slide and interpolating the pre-slide topography, using the intersection lines of interpolated structural features, based on geomorphic observations that included a careful observation of the structure/morphology of the mountain around. Calculation of the volumes and thickness of the slide involved measurement of the difference between pre- and post-slide DEM (Süzen and Doyuran, 2004).

Using the frequency ratio method and a logistic regression model (Esper Angillieri, 2010), relationships between the presence of debris rockslides and some variables were analyzed. Frequency ratio approaches are based on the observed relationships between distribution of debris – rockslides and each slide related variable, to reveal the correlation between debris – rockslides locations and the variables in the study area. Therefore, the frequency ratio can be calculated according to the following equation:

$$F_r = \frac{Ni}{N} \Big/ \frac{S_i}{S}$$

where S is the total number of pixels, N is the number of pixels with debris – rockslides occurrences; S_i is the number of pixels the i variable and Ni is the number of pixels in which the debris rockslides occurred in the i variable. If the value is greater than 1, it means a higher correlation, and a value smaller than 1 means lower correlation.

Logistic regression allows forming a multivariate regression relation between a dependent variable and several independent variables (Atkinson and Massari, 1998). The dependent data is made up of 0 and 1 values which show the absence and presence of debris rockslides respectively. The advantages of logistic regression are: 1) each variable used can be either continuous or discrete, and 2) it does not necessarily have a normal distribution. In the present situation, the binary dependent variable represents the presence or absence of debris rockslides. The forward stepwise logistic regression was carried out to incorporate predictor variables with an important contribution to the presence of debris-rockslides. The higher the logistic regression coefficient, the higher impacts on slide occurrence can be expected. In a logistic regression analysis, it is preferable that the number of pixels representing areas with an occurrence and that without it should be the same (Süzen and Doyuran, 2004a; Ayalew and Yamagishi, 2005).

In the study area, 200 points, on the rupture zone (exclude both the transport and the deposition of landslide), represent the debris rockslides. Therefore, 200 points without debris rockslides were randomly selected for logistic regression. The lithologic units and distances to lineaments classes were treated as categorical variables, and slope, aspect and elevation, as continuous variables. In logistic regression, multicollinearity checking is necessary to check the correlation of independent variables (Hosmer and Lemeshow, 1989). Multicollinearity is a statistical situation in which two or more predictor variables are highly correlated, meaning that one can be linearly predicted from the others with a non-trivial degree of accuracy. Tolerance (TOL) and the variance inflation factor are two important indexes that are widely used for multicollinearity checking. According to Menard (1995), a TOL value less than 0.2 is one indicator for multicollinearity, and serious multicollinearity occurs between independent variables when the TOL values are smaller than 0.1. The variance inflation factor (VIF) is calculated by 1/tolerance. If VIF value exceeds 10, it is often regarded as indicating multicollinearity. Additionally, the Pearson correlation was also used to test the correlation between variables.

4. Results and discussion

A total of 35 dry debris-rockslides were identified (Fig. 1), which covered an area of 6.36 km^2, accounting for 2.21% of the study area, with a total volume of 23.99×10^6 m^3. The minimum, mean and the maximum slide areas are 0.001, 0.18, and 0.66 km^2 respectively. Mean width of the rupture zone (Wr) is 301.30 m, and the mean length of the displaced mass (L_d) 373.22 m. The widths of the rupture zone (Wr) of individual debris-rockslides range from 28.21 to 1059.82 m and displaced mass (L_d) from 21.36 to 1197.95 m. Geometric characteristics of the individual debris-rockslides observed within the study area are presented in Table 1. Fig. 1 shows the spatial distribution of the debris-rockslides.

The volume of all debris rockslides was calculated from a DEM with low horizontal and vertical resolution (30 m), which

Table 1
List of debris-rock slide studied in the area and their attributes and morphological parameters.

Id	*P* [m]	Ad [km^2]	At [km^2]	Altitude [m asl]		Slope [degree]	Slope aspect	L [m]	Ld [m]	dr/Lr	Dd [m]	Wr [m]	Wd [m]	Hr [m]	V [m^3 E6]
				H_{max}	H_{min}										
1	1289.83	0.0897	0.11	3056	2944	24.01	SSE	275.27	228.93	0.15	15.08	377.69	429.57	112	0.1932
2	481.51	0.0150	0.0278	3050	2933	49.01	NNE	154.99	48.37	0.18	5.57	180.12	186.98	117	0.1064
3	3215.09	0.3854	0.5047	3354	2831	24.81	E	1254.85	1034.17	0.13	39.25	699.90	658.38	523	1.7127
4	1838.98	0.1195	0.1568	3147	2741	41.20	ESE	616.33	452.91	0.26	23.09	340.16	305.25	406	0.6105
5	91.85	0.0006	0.0011	2764	2747	27.24	ENE	37.14	21.36	0.13	2.59	31.58	32.71	17	0.0012
6	105.18	0.0007	0.0012	2814	2800	22.97	ENE	35.88	25.84	0.15	1.80	31.53	30.96	14	0.0005
7	1765.05	0.1345	0.1500	3128	2779	34.46	ENE	616.84	547.41	0.33	8.02	344.15	242.42	349	0.6114
8	760.57	0.0336	0.0543	3246	3101	19.35	ENE	332.02	186.05	0.25	12.39	171.46	204.59	145	0.2174
9	809.39	0.0422	0.0698	2924	2771	25.34	ENE	357.39	324.26	0.18	1.74	156.05	178.47	153	0.2860
10	155.79	0.0011	0.0019	2940	2905	66.11	ENE	38.28	32.22	0.32	4.06	28.21	31.67	35	0.0019
11	452.09	0.0096	0.0119	2943	2788	44.88	E	219.65	193.92	0.23	2.31	72.13	59.59	155	0.0277
12	181.70	0.0015	0.0046	3075	3008	41.02	ESE	144.75	71.22	0.27	1.80	30.30	41.80	67	0.0021
13	183.22	0.0014	0.0046	3075	3013	48.64	ESE	155.88	114.50	0.28	1.50	50.57	48.41	62	0.0015
14	976.20	0.0563	0.0784	3231	3095	24.72	SE	325.12	251.37	0.32	6.21	245.63	258.12	136	0.6391
15	896.70	0.0442	0.0493	3043	2880	41.23	NE	247.32	226.32	0.32	6.19	217.01	194.78	163	0.1461
16	2163.25	0.2654	0.3438	3252	2884	31.04	ENE	713.49	564.42	0.32	27.55	530.00	489.30	368	2.9666
17	1341.67	0.0938	0.1034	3441	3175	28.28	ESE	561.28	527.14	0.16	6.82	181.58	226.44	266	0.8310
18	277.12	0.0045	0.0077	3378	3275	43.77	SE	148.88	90.14	0.33	2.45	76.16	65.25	103	0.0022
19	264.40	0.0048	0.0079	2991	2918	54.97	E	77.79	59.86	0.33	7.35	77.35	96.25	73	0.0127
20	2959.78	0.3678	0.5302	3092	2522	33.84	ENE	1023.64	872.15	0.28	40.00	560.26	528.99	570	2.8503
21	3633.27	0.3566	0.5555	3330	2661	26.10	N	1375.22	1197.95	0.33	25.20	858.42	417.62	669	0.2323
22	415.54	0.0105	0.0131	3334	3178	43.32	ENE	165.41	144.10	0.26	23.15	90.86	72.50	156	0.0294
23	295.76	0.0040	0.0057	3186	3092	34.67	ENE	135.90	107.84	0.32	8.55	83.14	46.32	94	0.0106
24	758.84	0.0314	0.0349	3259	3111	24.92	E	318.55	292.32	0.27	22.88	113.06	119.66	148	0.1029
25	1631.10	0.1572	0.2542	3334	2948	30.16	ENE	664.22	571.83	0.30	68.50	402.07	309.33	386	1.7794
26	1025.24	0.0761	0.0913	2950	2732	31.90	SE	350.21	285.85	0.31	59.17	234.85	276.13	218	0.2236
27	2184.05	0.3010	0.4544	3666	3342	23.48	E	745.97	469.78	0.25	135.00	740.97	783.71	324	1.0861
28	2698.18	0.4331	0.6383	3772	3173	27.16	E	1167.73	613.09	0.29	111.78	432.56	786.19	599	3.6956
29	1452.09	0.1476	0.1780	3577	3260	33.45	E	479.77	333.15	0.29	59.82	296.61	430.78	317	0.6721
30	3092.62	0.4051	0.5553	3773	3229	25.29	ESE	1151.20	873.31	0.31	53.28	545.39	583.27	544	1.1999
31	2369.20	0.2071	0.3711	3937	3468	26.18	SE	954.06	658.70	0.33	51.19	521.37	342.61	469	0.7924
32	3279.65	0.3600	0.6658	3797	3276	31.21	SE	860.02	610.05	0.25	38.74	1059.82	796.01	521	1.1171
33	641.36	0.0269	0.0716	3508	3311	33.54	E	297.21	123.87	0.28	20.56	285.63	256.31	197	0.1544
34	534.38	0.0191	0.0422	3086	3021	14.29	E	255.13	195.66	0.14	16.67	240.59	102.85	65	0.0320
35	1805.60	0.2021	0.2139	4069	3755	24.14	WNW	767.87	712.72	0.16	54.22	238.26	359.17	314	1.6451

prevents correct volume analyses. A similar method of topographical reconstruction has been presented by Oppikofer (2009).

The 35 debris rockslides mapped were predominantly controlled by bedding planes. Cataclinal dip slope debris rockslides sensu Cruden (2000) are widespread in the study area, where slope angles are close to the bedding plane dip angle as it was observed by Cruden (1976) studies in Kananaskis Country in the southern Rockies. Debris rockslides are also common near resistant geological contacts, usually massive cliff-forming sandstone units or thick, resistant clastic units overlie recessive (less competent) clastic rocks. The bedrock geology of the rock slopes are sandstones and lutites of Ordovician and Silurian-Devonian age. All these rocks are strongly folded and faulted. In all the studied debris rockslides the movement was a typical rotational block sliding sensu Skempton and Hutchinson (1969) with a ratio Dr/Lr, between 0.1 and 0.3, and a slide body consisting of debris and rocks mass blocks.

The observed distribution of the debris rockslides, the frequency ratio and logistic regression coefficients are shown in Table 2. The variables were converted to a raster grid with 30 × 30 m cells. The area grid was 562 rows by 637 columns (i.e., total number is 355,885) and 2422 cells represent the rupture zone. The variables chosen and the system constructed were found to be valid; with 84% of the pixels used being correctly predicted (97% of the pixels of the debris-rockslides and 71% of non-slides). The test showed that the goodness of fit of the equation could be accepted because the values of Cox and Snell R2 (0.433) and Nagelkerke R2 (0.577) are greater than 0.2 (Clark and Hosking, 1986). The TOL, VIF values, and Pearson correlations in this study are shown in Table 3. There is no multicolinearity between any of the variables, which are weakly correlated with each other. The highest correlation was found between lithology and slope (−0.606) but its value is below the risk level of 0.7 (Clark and Hosking, 1986).

Table 2
Multicollinearity checking and Pearson's correlation coefficients between variables.

	Tolerance (TOL)	Variance inflation factor (VIF)	Elevation	Aspect	Slope	Lithology	Distances to lineaments
Elevation	0.811	1233	1000	−0.028	0.223	−0.416	−0.141
Aspect	0.966	1035	−0.028	1000	−0.140	0.107	0.128
Slope	0.620	1614	0.223	−0.140	1000	−0.606	−0.123
Lithology	0.547	1828	−0.416	0.107	−0.606	1000	0.065
Distances to lineaments	0.955	1047	−0.141	0.128	−0.123	0.065	1000

Table 3
Frequency ratios and logistic regression coefficients for different variables.

Variable	Class	N° de pixels showing slide occurrence[a]	% of pixels showing slide occurrence[b]	Pixel in domain[c]	Pixel %[d]	Frequency ratio[e]	Coefficients of logistic regression
Aspect [degree]	−1	0	0.000	30	0.008	0.000	
	315 − 45	305	12.593	82,050	23.055	0.546	
	45 − 135	1849	76.342	140,428	39.459	1.935	0.989
	135 − 225	259	10.694	75,615	21.247	0.503	
	225 − 315	9	0.372	57,762	16.231	0.023	
Elevation [m asl]	2031 − 2500	0	0.000	53,593	15.059	0.000	
	2500 − 3000	265	10.941	122,225	34.344	0.319	1.000
	3000 − 3500	1291	53.303	145,257	40.816	1.306	
	3500 − 4311	866	35.756	34,810	9.781	3.656	
Lithology	limestone and dark lutite	0	0.000	27,089	7.612	0.000	0.432
	sandstones and lutites	2422	100.000	202,159	56.805	1.760	1.064 E9
	conglomerate. sandstones	0	0.000	42,539	11.953	0.000	1.111
	conglomerates	0	0.000	2229	0.626	0.000	1.328
	colluvial-alluvial deposits	0	0.000	71,834	20.185	0.000	0.435
	unconsolidated deposits	0	0.000	10,035	2.820	0.000	0.000
Slope [degree]	0 − 15	177	7.308	157,573	44.276	0.165	
	15 − 25	998	41.206	106,505	29.927	1.377	1.038
	25 − 35	1069	44.137	78,407	22.032	2.003	
	35 − 57	178	7.349	13,400	3.765	1.952	
Distances to lineaments [m]	0 − 500	238	9.827	118,747	33.367	0.295	0.897
	500 − 1500	1199	49.505	153,411	43.107	1.148	2.215
	1500 − 2500	834	34.434	62,618	17.595	1.957	1.862
	2500 − 3500	151	6.235	20,436	5.742	1.086	0.000
	3500 − 4000	0	0.000	673	0.189	0.000	0.000

Total number of pixels showing slide occurrence = 2422.
Total number of pixel in domain = 355,885.
b = (a/2422) * 100.
d = (c/355,885) * 100.
e = b/d.

The area was divided into four elevation classes. The elevation map (Fig. 2) reveals that elevation ranges from 2031 to 4311 m asl. More than 89% of the debris-rock slides falls in the elevation interval ranging from 3000 to 4311 m a.s.l. (categories 3 and 4), with a frequency ratio of 1.306 and 3.656 which means a higher correlation but with a coefficient of logistic regression of 1.000, signals of low elevation influence.

Aspect regions (Fig. 2) were classified according to the aspect class as flat (−1°), north (315°–360°, 0°–45°), east (45°–135°), south (135°–225°) and west (225°–315°). More than 76% of debris rockslides fall within the quadrants represented the east category aspect (Table 2), with a frequency ratio of 1.935 (higher correlation) and a coefficient of logistic regression of 0.989. This means an influence of aspect on debris rockslide.

The slope angle map (Fig. 2) was divided into four slope classes: (a) flat to gentle slope (0°–15°), (b) moderate slope (15°–25°), (c) fairly moderate slope (25°–35°), (d) steep slope to very steep slope (35°–57°). The slide percentage in each slope class is presented in Table 2. This table indicates that most of the debris rockslides occur at slope angle between 15° and 35°, with a frequency ratio of 1.375 and 2.003, which indicates a higher correlation and coefficients of logistic regression of 1.038.

Six lithological units (Fig. 2) were differentiated depending on the rock type. The units included (1) limestone and dark lutite, (2) sandstones and lutites, (3) conglomerate, sandstones and argillite, (4) conglomerates, (5) colluvial-alluvial deposits and (6) Unconsolidated modern deposits, sand, silt and clay. All the debris rockslides observed in the area occurred in the unit number 2 (Table 2) which means that sandstones and lutites are the most influent lithology-type.

An examination of the distances to lineaments map (Fig. 2 and Table 2) reveals that most debris rockslides (about 59%) occur less than 1500 m from the lineament. However, no accuracy constraint exists for the position of the faults which were mostly extracted from morphological interpretation. However, the study area and its vicinity are significantly affected by the Neotectonic activity of the region (Perucca and Onorato, 2011).

Although there is a lack of numerical dating evidence, the debris rockslides can be assigned to mid-late Quaternary based on their physical location in the landscape and relative degree of preservation (accumulation and depletion zone preserved, well preserved failures). The role of rainfall as landslide trigger is acknowledged. However, while there is no doubt that precipitation has a major role in initiating slope failures in the surroundings of the study area (Esper Angillieri, 2011), the abundant earthquakes and very active faults (Perucca and Onorato, 2011; Esper Angillieri and Perucca, 2013) in the area have a key role to play. Hence, it is possible to conclude that the debris rockslides may have been triggered by high magnitude earthquakes, as was previously observed by Hermanns et al. (2001), who had argued that most of the landslides of central-western Argentina were seismically triggered.

5. Conclusion

Through high resolution satellite imagery interpretation, 35 debris rockslides were identified. In all debris rockslides, the lithology (sandstones and lutites) acts as the main controlling factor. A seismic origin related to Qauternary faults is proposed as the triggering factor of landslides in the area. Nevertheless, it has not been possibly to clearly relate a single slide to a certain trigger event or fault. In this context, earthquakes should be considered as a primary triggering factor for slide occurrence rather than precipitation in the study area.

The statistical analysis revealed that the distribution of debris rockslides can be explained mainly by lithology, with some additional influences of elevation and aspect. All debris rockslides lie above 2500 m a.s.l. with east facing aspect and slope angle between 15° and 35°.

The results obtained in this study have provided an advanced knowledge of the distribution of debris rockslides in the Precordillera of San Juan. Furthermore, the methodology presented here is easy to reproduce and may be applied to other mountainous regions. Finally, this finding confirmed that several of the chosen variables played a dominant role in controlling the spatial distributions of the debris rockslides.

Acknowledgements

The author thanks especially the anonymous reviewer for his helpful comments. Finally, the author acknowledges funding received from CONICET (Argentinean National Council of Scientific and Technological Research) and CICITCA (Secretary of Science and Technology UNSJ) to support this research.

References

Allmendinger, R., Figueroa, D., Snyder, D., Beer, J., Mpodozis, C., Isacks, B., 1990. Foreland shortening and crustal balancing in the Andes at 30°S latitude. Tectonics 9 (4), 789–809.
Atkinson, P.M., Massari, R., 1998. Generalised linear modelling of susceptibility to landsliding in the central Appenines, Italy. Computers and Geosciences 24 (4), 373–385.
Ayalew, L., Yamagishi, H., 2005. The application of GIS-based logistic regression for landslide susceptibility mapping in the Kakuda-Yahiko Mountains, Central Japan. Geomorphology 65, 15–31.
Clark, W.A.V., Hosking, P.L., 1986. Statistical Methods for Geographers. Wiley, New York, p. 520.
Cruden, D.M., 1976. Major rock slides in the Rockies. Canadian Geotechnical Journal 13, 8–20.
Cruden, D.M., 2000. Some forms of mountain peaks in the Canadian Rockies controlled by their rock structure. Quaternary International 68–71, 59–65.
Dikau, R., 2004. Mass movement. In: Goudie, A.S. (Ed.), Encyclopedia of Geomorphology, vol. 2. Routledge, London, pp. 644–653.
Esper Angillieri, M.Y., 2010. Application of frequency ratio and logistic regression to active rock glacier occurrence in the Andes of San Juan, Argentina. Geomorphology 114 (3), 396–405.
Esper Angillieri, M.Y., 2011. Inventario de Procesos de Remoción en masa en un sector del Departamento Iglesia, San Juan, Argentina. Revista de la Asociación Geológica Argentina 68 (2), 225–232.
Esper Angillieri, M.Y., 2012. Análisis de la vulnerabilidad por flujos en masa en la Provincia de San Juan (Oeste de Argentina). Revista de la Sociedad Geológica de España 25 (3–4), 145–156.
Esper Angillieri, M.Y., Perucca, L.P., 2013. Mass movement in Cordón de las Osamentas, de La Flecha river basin, San Juan, Argentina. Quaternary International 301, 150–157.
Esper Angillieri, M.Y., Perucca, L., Rothis, M., Tapia, C., Vargas, N., 2014. Morphometric Characterization and Seismogenic Sources Relationships of a Large Scale Rockslide. Quaternary International 352, 92–99.
Fauqué, L., Cortés, J.M., Folguera, A., Etchverría, M., 2000. Avalanchas de rocas asociadas a neotectónica en el valle del río Mendoza, al sur de Uspallata. Revista Asociación Geológica Argentina 55 (4), 419–423.
Fell, R., Corominas, J., Bonnard, C., Cascini, L., Leroi, E., Savage, W.Z., 2008. Guidelines for landslide susceptibility, hazard and risk zoning for land-use planning. Engineering Geology 102, 99–111.
Fernández, D.S., 2005. The giant paleolandslide deposits of Tafí del Valle, Tucumán Province, Argentina. Geomorphology 70, 97–111.
González Díaz, E.F., 2009. Deslizamientos al norte de la población de Tricao Malal, noroeste de Neuquén. Revista de la Asociación Geológica Argentina 65 (3), 545–550.
González Díaz, E.F., Folguera, A., 2009. Los deslizamientos de la cordillera neuquina al sur de los 38° S: su inducción. Revista de la Asociación Geológica Argentina 64 (4), 569–585.
Hermanns, R.L., Niedermann, S., Villanueva García, A., Sosa Gómez, Strecker, M.R., 2001. Neotectonics and catastrophic failure of mountains fronts in the southern intra-Andean Puna Plateau, Argentina. Geology 29 (7), 619–623.
Hosmer, D.W., Lemeshow, S., 1989. Applied Logistic Regression. John Wiley & Sons, Inc, New York, p. 307.
IAEG, 1990. Suggested nomenclature for landslides. Bulletin of the International Association of Engineering Geology 41, 13–16.
Menard, S.W., 1995. Applied Logistic Regression Analysis. SAGE, Thousand Oaks, p. 128.
Moreiras, S.M., Coronato, A., 2009. Landslide processes in Argentina. Developments in Earth Surface Processes 13, 301–332.
NASA, 2011. ASTER Global Digital Elevation Map V2. http://gdem.ersdac.jspacesystems.or.jp.
Oppikofer, T., 2009. Detection, Analysis and Monitoring of Slope Movements by Highresolution Digital Elevation Models (Ph.D. thesis). Institute of Geomatics and Analysis of Risk, University of Lausanne, Lausanne, Switzerland.
Perucca, L.P., Esper Angillieri, M.Y., 2008. La avalancha de rocas Las Majaditas. Caracterización geométrica y posible relación con eventos paleosísmicos. Precordillera de San Juan, Argentina. Revista Española de la Sociedad Geológica de España 21 (1–2), 35–47.
Perucca, L.P., Esper Angillieri, M.Y., 2009a. El deslizamiento de rocas y detritos sobre el río Santa Cruz y el aluvión resultante por el colapso del dique natural, Andes Centrales de San Juan. Revista de la Asociación Geológica Argentina 65 (3), 571–585.
Perucca, L.P., Esper Angillieri, M.Y., 2009b. Evolution of a debris-rock slide causing a natural dam: the flash flood of Río Santa Cruz, Province of San Juan. November 12, 2005. Natural Hazards 50 (2), 305–320.
Perucca, L.P., Onorato, M.R., 2011. Fallas con actividad cuaternaria en el Corredor Tectónico Matagusanos –Maradona – Acequión entre los ríos de La Flecha y Del Agua. Provincia de San Juan. Revista de la Asociación Geológica Argentina 68 (1), 38–51.
SEGEMAR, 2000. Carta Geológica de la República Argentina. Hoja (3169-IV) San Juan, escala 1:250.000. Servicio Geológico Minero Argentino, Buenos Aires, p. 75.
Skempton, A.W., Hutchinson, J.N., 1969. Stability of natural slopes and embankment foundations. In: Proceedings of the 7th International Conference on Soil Mechanics and Foundation Engineering. Sociedad Mexicana de Suelos, Mexico City, pp. 291–340. State of the Art Volume.
Süzen, M.L., Doyuran, V., 2004. Data driven Bivariate landslide susceptibility assessment using geographical information systems: a method and application to Asarsuyu catchment, Turkey. Engineering Geology 71 (3–4), 303–321.
Vittorio De Blasio, F., 2011. Introduction to the Physics of Landslides. Springer, Dordrecht Heidelberg London New York, p. 408.